Simulation of a floating solar farm in waves with a novel sun-tracking system

Yujia Wei[1], Binjian Ou[1], Junxian Wang[1], Liang Yang[1], Zhenhua Luo[1], Sagar Jain[1], Wolter Hetharia[2], Soegeng Riyadi[3], IKAP Utama[3] and Luofeng Huang[1]*

[1]School of Water, Energy and Environment, Cranfield University, Building 52, Cranfield, 45 College Rd, Cranfield, MK43 0AL UK
[2]Department of Naval Architecture, University of Pattimura, Ambon, 97223, Indonesia
[3]Department of Naval Architecture, Institut Teknologi Sepuluh Nopember, Surabaya, 60111, Indonesia
*luofeng.huang@cranfield.ac.uk

Abstract. The awareness of the energy and climate crisis has accelerated the development of renewable energy sources. Photovoltaic (PV) solar power plants harvest clean solar energy and convert it to electricity, which will be one of the most promising alternatives to the power industry in the context of a low-carbon society. Due to its low power density, the traditional deployment of PV systems on land or inland rivers requires much space. Therefore, industries are increasingly interested in expanding offshore Floating PhotoVoltaics (FPV) to oceans, where FPV has less influence on the marine environment and does not occupy precious space for land resources and human activities. This study performs a hydrodynamics-based structural response analysis for a novel FPV system in OpenFOAM. The wave-proof FPV platform is newly designed for this work, which integrated breakwater technologies to sustain the system's survivability in harsh ocean-wave environments. Firstly, the rational mooring types for FPVs installed close to the island are studied considering seabed effects. Subsequently, extensive parametric studies have been conducted to determine a rational design strategy for the mitigation of wave impact. Several potential effects of the proposed platforms on the hydrodynamics in a coastal sea are evaluated for the first time.

1. Introduction

The Floating PhotoVoltaic system (FPV) has garnered significant interest in the industry due to its unique combination of extendable PV size and floating structure benefits. By utilizing a floating structure, the system can absorb solar radiation energy, which reduces temperature and ultimately improves efficiency. The efficiency of floating solar plant is 11% higher than the conventional solar power plant and reduces the water evaporation by 70%, however, the investment of such power plant is 1.2% higher [1]. The development of FPV is particularly important in areas that lack land and lake space. Some review papers have addressed for FPV development, such as, FPV installation guidelines [2], general FPV technologies [3], Hybrid FPV system that combins with other renewable energy sources [4] and the economic aspects of FPV systems [5], to name a few. Several design regulations for the FPV system have been given by DNV GL [6].

Despite previous efforts, the development of FPV systems has remained limited to calm or near-shore regions, with offshore development still in the trial and design stage. The unpredictable ocean environment restrains the development of FPV systems in deep-sea regions. Because PV panels are relatively fragile, the platform design should support them and prevent wave attacks. Some pioneering

industrial designs, such as those from Ocean Sun [7] and Oceans of Energy, have shown promising field test results. As reported by Oceans of Energy [8], the FPV prototype test in the North Sea Two (NS2) [9] project successfully operated in offshore regions for 11 months. During this time, it withstood storms such as "Ciara," "Dennis," and "Bella," with maximum wave heights of 13.5m.

Parallel with the experimental investigations numerical simulations were developed to predict the dynamics structure motions of the FPV system in waves. Choi, Park [10] conducted a series of simulations to investigate the motions and stress distributions of a floating PV system based on a one-way coupled CFD and FEA simulation with various inlet angles of wind and wave loads. The authors found that the first or last row of solar panels in a solar farm was exposed to the highest wind loads and stress. The drawback of this method is the pressure distributions on the solar panel were measured in the steady state conditions. As a recommendation for future work, the transient analysis of pressure distributions on solar panel should be studied in transient state. Song, Kim [11] presented a global performance analysis for a moored FPV system based on a combination of software. The selected FPV system consists of 100 floating modules and the whole system is tested in an inner harbour, and the wave height was set to 1.5m as the severe condition. The large scale effects of the FPV system were studied and the results showed that the largest motions and shear forces are detected at the corner modules. The reinforcements of the frame at the corner should be applied.

Based on the lessons learned from previous studies, a novel solar farm concept is proposed in this study, takeing two primary advantages: 1) A hexagonal shape breakwater is designed for the solar farm to avoid direct contact from all-directional waves. 2) A installation of a sun-tracking system that rotates the solar farm to maximise the overall energy production.

The tracking system in floating is easier to implement than that in ground . This is because PV panels float on water hence it requires little energy to rotate the whole structure. The tracking system in FPV consists of a rotary structure to track the azimuth angle and a tilt variable structure to track the tilt angle. The pinoneering prototype from K-water (Korea Water Resources Corporation) has installed the world's first 100 kW tracking-type floating photovoltaic generation system in Korea for commercial power generation [12]. The tracking system has evidence that it will cost 1% of the total energy output and give a 10% of the energy feedback.

In this context, the present study fills in the gap that no research has investigated on the dynamic behaviours of a rotary solar farm in waves based on a fully nonlinear CFD method. The computational results, including the breakwater performance and the dynamic behaviors of the FPV system with/without mooring lines, are presented.

This paper is structured as follows: in Section 2, the problem definition on the solar farm is discussed. In Section 3, the numerical setting ups and methodology used are presented. In section 4, the simulation results of the solar farm with/without a mooring system are illustrated accordingly. Section 5 summarises this work with its main conclusions.

2. Problem definition

The prototype design of the novel offshore solar farm consists of three parts: an octagonal shape of breakwater, a rotary PV supporting structure and a mooring system, as shown in Figure 1. The breakwater is designed to protect the platform from all-directional waves and currents. The rotary PV supporting structure is where the photovoltaic panels are installed, and it rotates relatively to the breakwater with the rotational speeds controlled by the tracking system. The mooring system keeps the platform anchored in place.

This innovative design allows for scalability and flexibility in energy output. The designed energy output of a single moduluar is a 1MW with a 100m in diameter, and it has the capacity to extend to 4MW by connecting multiple modules together using a hard or soft connection, as shown in Figure 1(b). The middle region of the four modules can be designed to house an energy conversion and storage system. This system can include energy storage options such as batteries, along with a conversion system that can efficiently transfer energy to the grid.

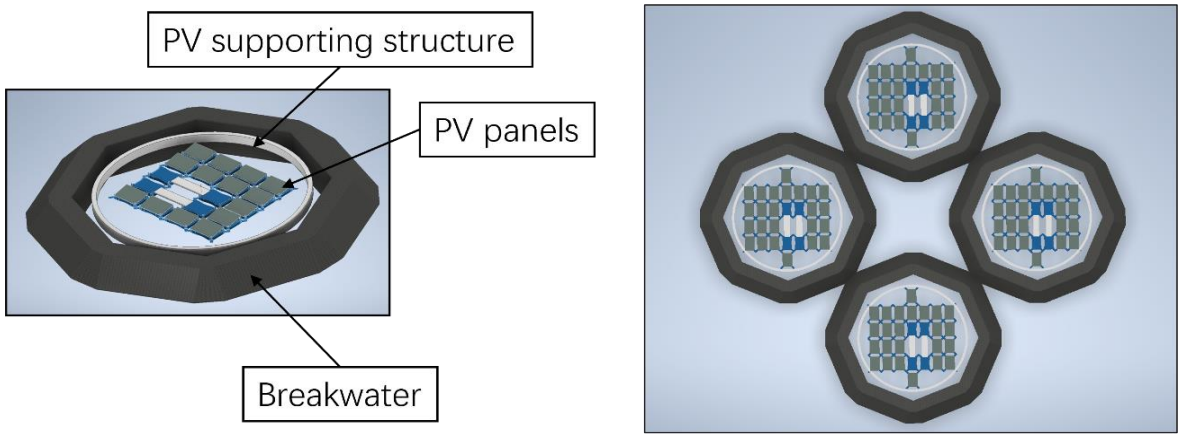

(a) (b)

Figure 1. The configuration of the FPV solar farm: (a) Single modular design, (b) multiple modular design.

The FPV platform is equipped with a tracking system that ensures a constant rotational speed. The active control system is currently in place to ensure that the platform functions smoothly, as shown in Figure 2(a-c). However, as technology advances and evolves, a passive control system (Figure 2d) can be implemented in the future. This would allow for a more efficient and streamlined approach to the management of the platform.

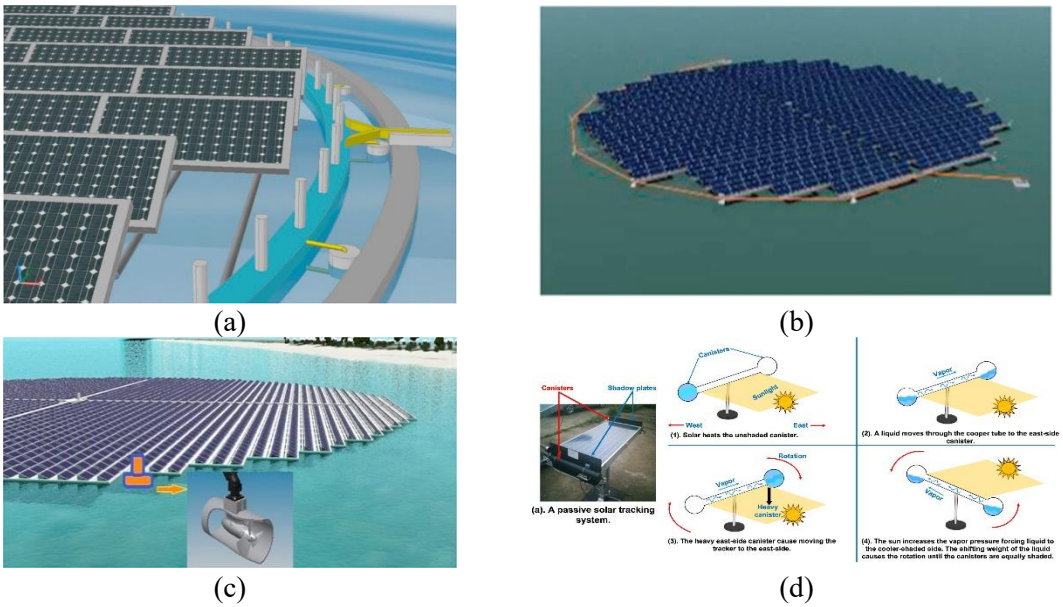

(a) (b)

(c) (d)

Figure 2. Tracking system used on solar farms: (a) Tracking with a confining structure [13], (b) rope system [13], (c) bow thrusters [13], (d) passive tracking [14].

3. Computational approach

In this study, a numerical framework is presented to investigate the dynamic motions of a rotary solar farm with a tracking system in waves based on the open-source toolbox OpenFOAM. The flow field is

calculated by solving the Navier-Stokes equations, while the structure motions are calculated by rigid body assumptions. The relative rotation between the PV supporting structure and breakwater is accounted for using the nested sliding mesh technique in OpenFOAM. The catenary shape mooring lines and their effects on the structural motions are evaluated by a quasi-static method. The detailed numerical principles of each are described in the following sub-sections.

3.1. Governing equations

The governing equations for a transient, incompressible, and viscous fluid can be written as

$$\nabla \cdot U = 0 \tag{1}$$

$$\frac{\partial \rho U}{\partial t} + \nabla \cdot (\rho UU) - \nabla \cdot \tau = -\nabla P_d + \rho g + F \tag{2}$$

where U refers to the velocity of flow field, ρ is the mixed density of water and air, g is the gravity acceleration, P_d refers to the dynamic pressure, τ is the dynamic viscosity, F is the surface tension. The VOF technique was adopted to simulate the free surface using an additional transport equation to solve for the volume fraction *a.* The volume fraction a is assigned a value of 0 when the cells are filled with air, and a =1 the cell is filled with water.

3.2. Computational domain and mesh generation

The finite volume mesh is generated by the mesh generation tool "SnappyHexMesh" based on a cell splitting and body fitting technique in OpenFOAM. The model scale of solar farm geometry is used in this study, with a scale of 1:100 applied. The purpose of using a model scale is to validate the experimental data in future work. The wave domain extends in three directions, i.e., $-3.0L < x < 4.0L$, $-2.0L < y < 2.0L$ and $-4.0L < z < 1.5L$, where L refers to the characteristic length of the solar farm ($1.2m$), as shown in Figure 3(a). The mesh region at the free surface is progressively refined several times, however, the mesh uncertainty tests are not conducted in this study. The mesh region close to the structure requires a more refined mesh in the area immediately around the solar farm, as shown in Figure 3(b).

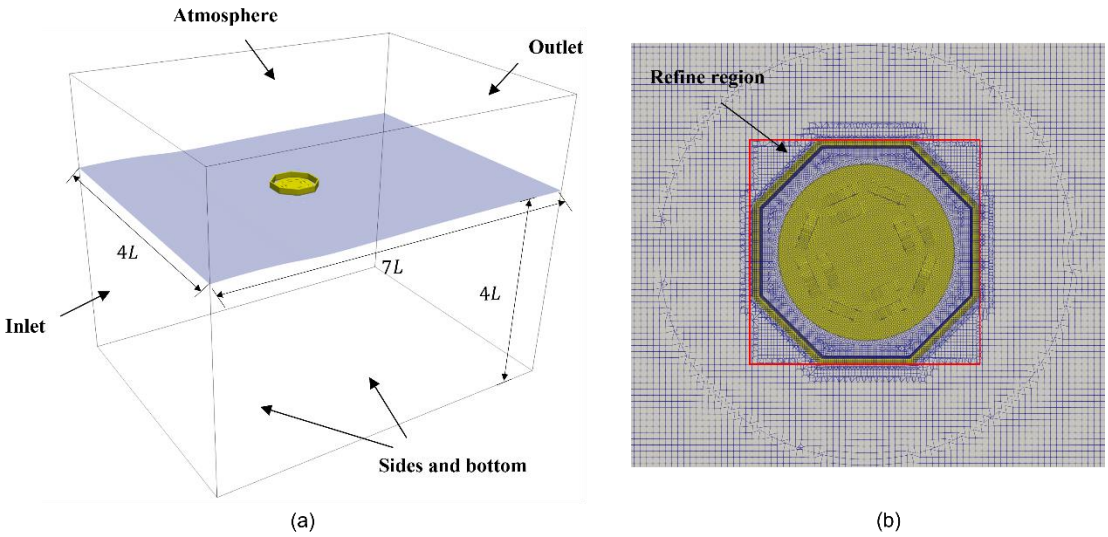

Figure 3. The layout of (a) the overall computational domain and (b) detailed mesh regions.

3.3. Boundary conditions

The boundary conditions for the wave-structure interaction problem are as follows: at the inlet on the left boundary, the velocity and alpha phases are prescribed as the incident waves. An in-house wave absorption boundary condition is used on the outlet side of the wave domain. The top domain is set as atmosphere, and the bottom of the domain is set as a symmetry plane, representing a deep-water condition. The moving wall boundary condition with zero pressure gradient is defined on the geometrical surface of the solar farm.

3.4. Wave generation and absorption

The wave generation library "waves2Foam" used in this study to generate the regular heading waves inside the wave domain [15]. The second order Stokes waves theory was used to generate the regular waves throughout all the cases with the following equations:

$$\eta = \frac{H}{2}\cos(\theta) + k\frac{H^2}{4}\frac{3-\sigma^2}{4\sigma^3}\cos(2\theta) \tag{3}$$

$$u = \frac{H}{2}\omega\frac{\cosh(kz)}{\sinh(kz)}\cos(\theta) + \frac{3}{4}\frac{H^2\omega k\cosh(2kz)}{4\sinh^4(kh)}\cos(2\theta) \tag{4}$$

$$w = \frac{H}{2}\omega\frac{\sinh(kz)}{\sinh(kz)}\sin(\theta) + \frac{3}{4}\frac{H^2\omega k\sinh(2kz)}{4\sinh^4(kh)}\sin(2\theta) \tag{5}$$

where, H is the wave height, wave angle $\theta = kx - \omega t + \psi$ with k is the wave number, ω is the angular frequency and ψ is the wave phase and $\sigma = \tanh(\mathrm{kh})$.

The relaxation zone technique is used to improve wave quality near the inlet boundary and eliminate spurious reflections at the outlet boundary. The primary function of the relaxation zones is specified by the following equations.

$$a_R(\chi_R) = 1 - \frac{\exp(\chi_R^{3.5}) - 1}{\exp(1) - 1} \tag{6}$$

$$\phi_R = \omega_R \phi_R^{computed} + (1 - \omega_R)\,\phi_R^{target} \tag{7}$$

where ϕ_R refers to either the velocity or volume fraction of water a. The definition of χ_R is that the weighting function a_R is always 1 at the interface between the non-relaxed computational domain and the relaxation zones, and χ_R is a value between 0 and 1.

3.5. Model description

3.5.1. Rigid body motion. In OpenFOAM, the global motion of a solar farm can be calculated based on the rigid body motion equations, which are written as follows:

$$H(q)\ddot{q} + C(q,\dot{q}) = \tau \tag{8}$$

where $q, \dot{q}, \ddot{q}$ denote as the position, velocity and acceleration of the structures, H is the inertia matrix, C is the force which produces zero acceleration, which accounts for forces like gravity, Coriolis and centrifugal forces, τ is the total force acting on the bodies. In this equation, multi-values can be calculated based on what has been provided. Therefore, the forward dynamics method is applied to calculate the acceleration based on the initial position, velocities and forces with the equations shown below:

$$\ddot{q} = FD(model, q, \dot{q}, \ddot{q}) \tag{9}$$

This calculated acceleration will be integrated for the first time step to get the new position and velocity, which will be used as input for the next time step. The forces at bodies are updated simultaneously. Boundary conditions can be applied to a rigid body by applying restraints (forces acting on the body) and constrained (the degree of freedom is restricted).

3.5.2. The nested-sliding mesh technique. The tracking system raise complexity in numerical modellings. To account for the relative rotation between the PV supporting structure and breakwater, the nested sliding mesh technique is applied in OpenFOAM. Two pairs of AMI (Arbitrary Mesh Interface) surfaces with three cell zones are defined accordingly, as shown in Figure 4. The outer cell zone completely covers the structure, allowing the solar farm to move globally in 6 DOF. The inner cell zone covers the PV supporting structure, allowing for relative rotational movement to the breakwater. AMI surfaces are sandwiched between three cell zones for data transmission and exchange. It is worth noting that the usage of nested sliding mesh should avoid any overlap or gap between each pair of AMI surface. Overall, the nested sliding mesh allows for the modelling of the solar farm global responses with free surface, self-rotations of PV supporting structure and their coupled motions. The rotary speed is controlled constant in this study.

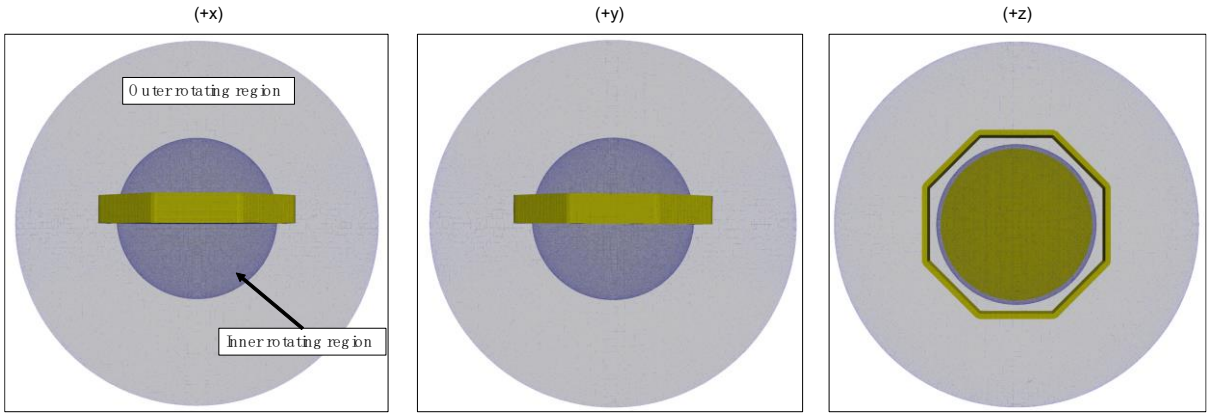

Figure 4. The layout of the nested sliding mesh and cell zone regions: (a) +x, (b) +y, (c) +z.

3.6. Mooring system

The mooring tension is calculated using the catenary equation, derived from [16]. Figure 5(a) shows the profile of a two-dimensional mooring line. The initial pretension is T_f at the top point of the line. The water depth, or the depth of the anchor point, is h. Quasi-static methods assume that the shape and tension of a mooring line at any given instant are static while ignoring the dynamic loadings from fluids.

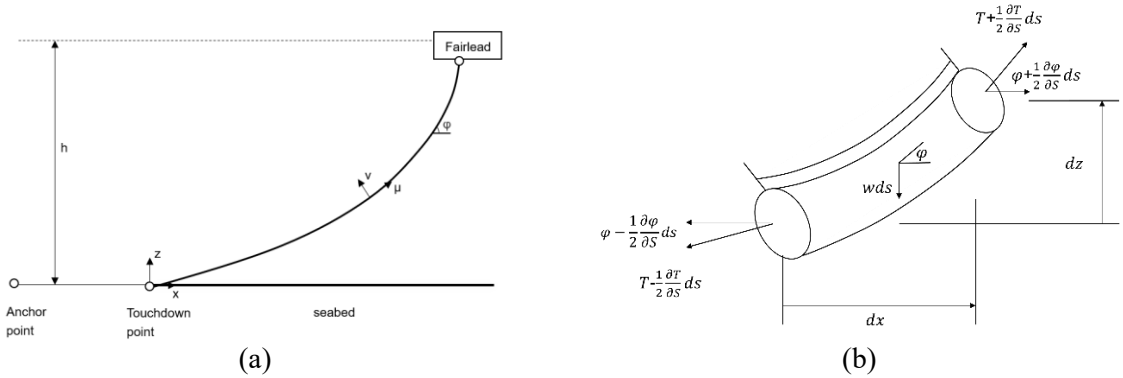

Figure 5. Illustration of the mooring modelling (a) The layout of catenary shape mooring lines, (b) An example of small segment of catenary mooring line.

An infinitely small element of mooring line is shown in Figure 5(b). In the absence of fluid forces, it is possible to resolve the forces acting normally and tangentially to the element with the following equations:

$$\frac{d\varphi}{ds} = \frac{w}{T}cos\varphi \tag{10}$$

$$\frac{dT}{ds} = wsin\varphi \tag{11}$$

where T is element's tension, w is submerged weight per unit length, φ is the angle between the axial and horizontal directions.

$$H = T_f - wh \tag{12}$$

$$L = h\sqrt{\frac{2T_f}{wh} - 1} \tag{13}$$

$$X = \frac{H}{w}cosh^{-1}(\frac{wh}{H} + 1) \tag{14}$$

$$V = wL \tag{15}$$

where L is the length of the line in its elongation under the given pretension T_f, X is the horizontal distance from touchdown point to fairlead, and V is the vertical force component at fairlead. The mooring line seabed interaction is modeled by a simplified spring damper model. When a node touches the seabed, a vertical reaction force is applied to that node. To obtain the tension force and coordinates of each node of a mooring line, the above equations are solved in a piecewise manner.

4. Results

In order to evaluate the performance of the solar farm, a series of numerical simulations were conducted in a regular heading wave with a frequency $f_w = 0.91Hz$ and a wave height $H_w = 0.10m$. The time step is selected as 0.005s through all simulations to ensure the model progress smoothly. The numerical results are presented in this section, including the analysis of the breakwater performance, tracking system evaluation and the dynamic motions of the solar farm with and without mooring lines.

4.1. Breakwater performance

The octagonal shape breakwater installed surrounding the PV supporting structures to absorb the wave energy and avoid direct contact between the structure and waves. Two wave gauges were placed: one in the wave propagation area and one between the breakwater and supporting structure. It was found that approximately 40% of wave heights are blocked due to the breakwater's design. However, breakwater performance cannot be accurately determined based on a simulation at a single frequency. It is worth repeating numerical models with different wave elevations and frequencies to properly evaluate breakwater performance.

4.2. Tracking motion visualization

An active control tracking system is installed for the solar farm. It allows for relative rotation between the breakwater and the PV supporting structure. The rotational speed for this design is modelled as 1 rad/s, but in reality it should be calibrated with the angle of sunlight radiation. Figure 6 shows screenshots of five rotating angles, from 45 to 135 degrees, taken at 5-second intervals over 25 seconds. Due to the relatively slow rotational speeds, the rotation of the structure may not have an effect on the surrounding flow field. However, the rotation of the upper PV panel will change the wind field, which is worth further investigation.

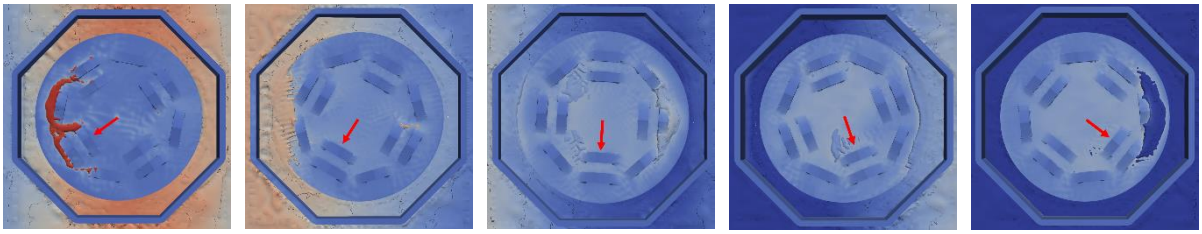

Figure 6. Virtual observation of the active control system.

4.3. Dynamic motion of solar farm

The dynamic response of the solar farm without a mooring system is evaluated at wave frequency $f_w = 0.91Hz$ and wave height $H_w = 0.10m$. The time-series heave and pitch motions are plotted in Figure 7. The signals have a main frequency component coincident with the wave frequency. However, there are also noticed nonlinearity components that may come from the implementation of breakwater. The three-dimensional virtual observation of the wave-structure interaction is shown in Figure 8.

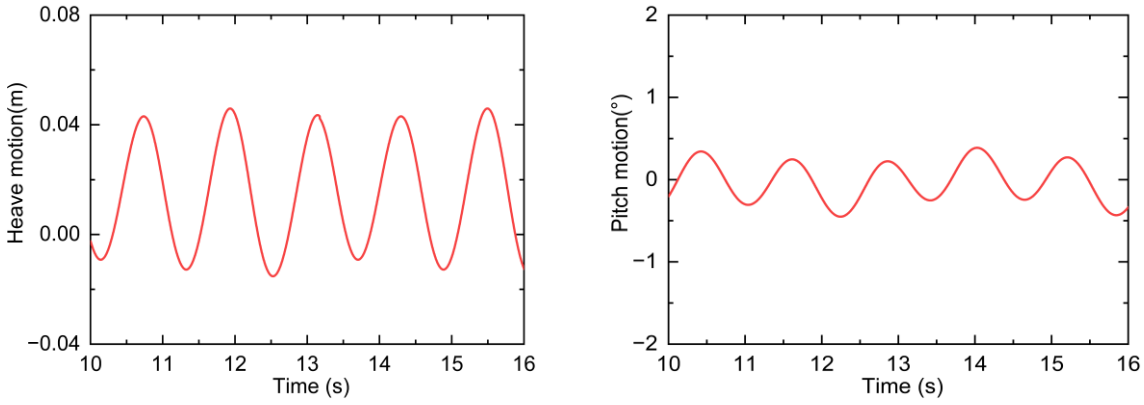

(a) (b)

Figure 7. Dynamic motion (heave and pitch) of the solar farm in regular heading waves: (a) Heave, (b) Pitch.

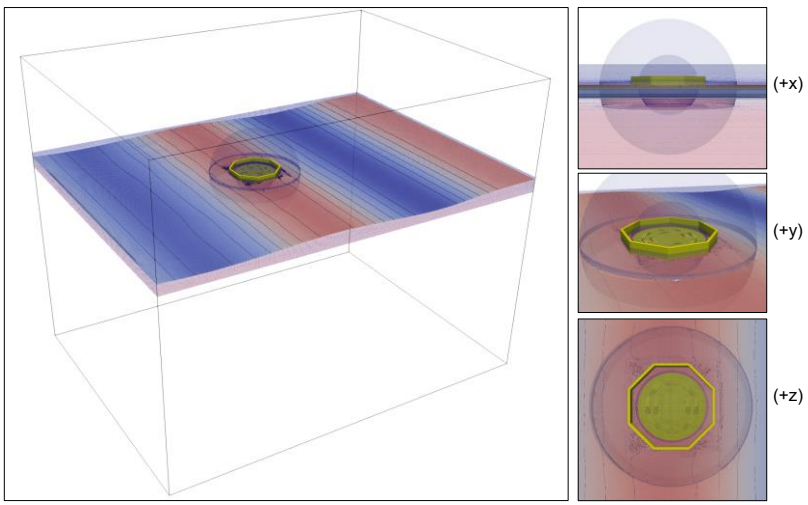

Figure 8. Virtual observation of the solar wave farm in waves.

4.4. FPV with catenary mooring system

The mooring system is essential in solar farm design, as it provides restoring forces and moments to balance environmental loadings and help maintain the farm's position at sea. In this study, the catenary type of mooring lines was implemented, which is suitable for floating structures operating in medium-deep water conditions. It consists of a chain or wire rope that hangs between the fairlead and anchor points, forming a curve known as the catenary. Eight catenary mooring lines, each with their fairleads attached to the vertex of the breakwater, distributed at a 45°angle, as shown in Figure 9. The overall length of the mooring lines is 7.8m, with 1.56m (8 segments) lying down on the seabed and 6.24m hung in water. The main mooring characteristics are summarized in Table 1.

Table 1: Properties of the catenary type mooring lines.

Properties	Value
Arrangement angle	45°
Mooring segment	40
Mooring length	7.8m
Mooring line diameter	3.656mm
Mooring line mass per unit length	0.0607
Mooring line stiffness	$2.78e^{6}$
Seabed stiffessnesss	$1e^{6}$

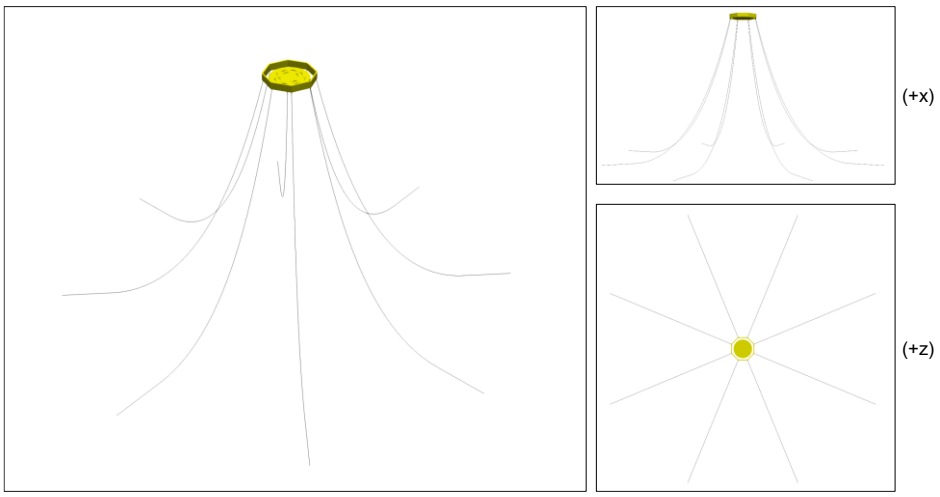

Figure 9. Catenary type of mooring system configuration of the proposed FPV platform.

Figure 10 compares the effects of attaching a mooring system on the structural motions of the solar farm. The stabilization provided by the mooring lines is particularly noticeable in pitch motions, where the peak magnitude is reduced by approximately 12.5%. However, heave motions are not significantly affected by the mooring lines, as catenary mooring lines restrain the structure through gravity. To achieve optimal performance of the mooring lines, an optimization procedure is required to determine their characteristics. This process involves a detailed analysis of the environmental conditions, including wind, waves, and currents, to ensure that the mooring system can withstand the expected loads.

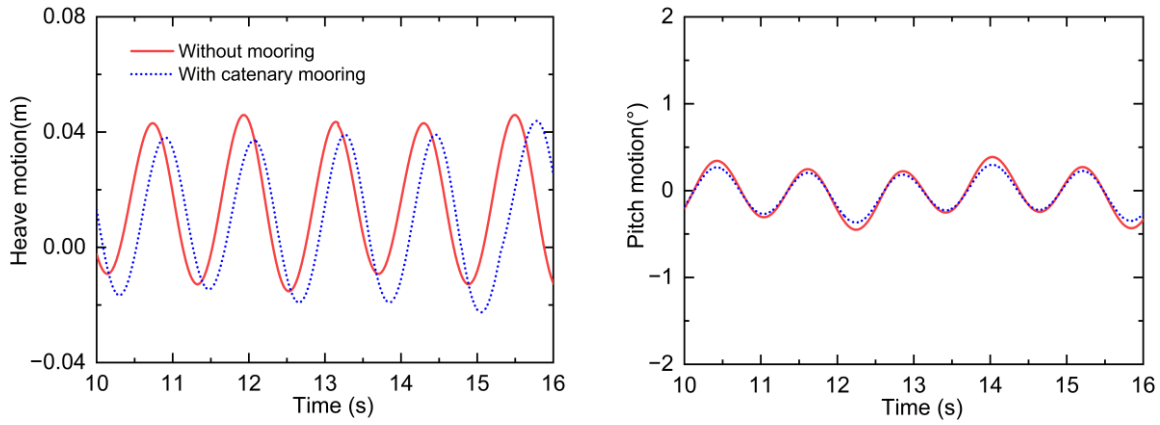

(a) (b)

Figure 10. Comparison on the vertical motions of the solar farm with and without mooring system: (a) Heave, (b) Pitch.

5. Conclusions

The development of offshore solar farms is a crucial step towards sustainable energy production. This paper presented a novel design for a solar farm that includes a breakwater, PV supporting structure, mooring system, and tracking system. This design has the potential to shed light on the industry for future prototype designs.

To study the dynamic motions of such a system in waves, high fidelity CFD methods are applied. Some important factors, including breakwater performance, dynamic motions with/without a mooring system, are studied. The main conclusions are outlined below:

- Designing breakwaters to avoid wave attacks is important for the FPV section, as it reduces the risk of damage due to rough seas.
- The tracking system should be modelled so that the PV supporting structure rotates along with the sun, improving conversion efficiency. This would ensure that the solar panels are always positioned to receive the maximum amount of sunlight.
- The mooring system should be carefully designed, as the catenary mooring lines tested in this paper, can effectively reduce the global pitch motion. This would minimize the amount of movement experienced by the solar farm so as to improve its stability.
- Experimental studies will be conducted in the future to validate the present CFD framework, using the wave tank facility at Cranfield University.

Acknowledgements

This work has been supported by funding from the Innovate UK “Solar2Wave” project (grant No. 10048187), The authors would like to acknowledge the usage of the Delta 2 High-Performance Computing based at Cranfield University.

Referencence

[1] Sahu A, Yadav N, and Sudhakar K, Floating photovoltaic power plant: A review. *Renewable and Sustainable Energy Reviews*, 2016. **66**: p. 815-824.
[2] Trapani K and Redon M, A review of floating photovoltaic installations: 2007-2013. *Progress in Photovoltaics*, 2015. **23**(4): p. 524-532.
[3] Essak, L and Ghosh A, Floating Photovoltaics: A Review. *Clean Technologies*, 2022. **4**(3): p. 752-69.
[4] Solomin E, Soritkin E, Cuce E, and Selvanathan S P, Hybrid Floating Solar Plant Designs: A

Review. *Energies*, 2021. **14**(10).
[5] Cazzaniga R and Rosa-Clot M, The booming of floating PV. *Solar Energy*, 2021. **219**: p. 3-10.
[6] DNVGL_AS, *Recommended Practice DNVGL-RP-0584: Design, Development and Operation of Floating Solar Photovoltaic Systems*. 2021: Technical Report.
[7] OceanSun. *https://oceansun.no/*. [cited 2023 10/04].
[8] Oceans_of_Energy. *https://oceansofenergy.blue.com*. 2020 [cited 2023 19/03].
[9] Safety4Sea, *Offshore floating solar farm installed at the Dutch North Sea*. 2020.
[10] Choi S M, Park C D, Cho S H and Lim B J, Effects of various inlet angle of wind and wave loads on floating photovoltaic system considering stress distributions. *Journal of Cleaner Production*, 2023. **387**.
[11] Song J, Kim J, Chung W C, Jung D, Kang Y J and Kim S, Wave-induced structural response analysis of the supporting frames for multiconnected offshore floating photovoltaic units installed in the inner harbor. *Ocean Engineering*, 2023. **271**.
[12] Choi Y K and Lee Y G, A Study on Development of Rotary Structure for Tracking-Type Floating Photovoltaic System. *International Journal of Precision Engineering and Manufacturing*, 2014. **15**(11): p. 2453-60.
[13] Cazzaniga R, Cicu M, Rosa-Clot M, Rosa-clot P, Tina G M and Ventura C, Floating photovoltaic plants: Performance analysis and design solutions. *Renewable and Sustainable Energy Reviews*, 2018. **81**: p. 1730-1741.
[14] El Hammoumi A, Chtita S, Motahhir S and El Ghzizal A. Solar PV energy: From material to use, and the most commonly used techniques to maximize the power output of PV systems: A focus on solar trackers and floating solar panels. *Energy Reports*, 2022. **8**: p. 11992-2010.
[15] Jacobsen N G, Fuhrman D R and Fredsøe J, A wave generation toolbox for the open-source CFD library: OpenFoam®. *International Journal for numerical methods in fluids*, 2012. **70**(9): p. 1073-1088.
[16] Ong P P and Pellegrino S. Modelling of seabed interaction in frequency domain analysis of mooring cables. in *International Conference on Offshore Mechanics and Arctic Engineering*. 2003.

Simulation of a floating solar farm in waves with a novel sun-tracking system

Wei, Yujia

2023-08-09

Wei Y, Ou B, Wang J, et al., (2023) Simulation of a floating solar farm in waves with a novel sun-tracking system, IOP Conference Series: Materials Science and Engineering, Volume 1288, August 2023, Article Number 012041

https://doi.org/10.1088/1757-899X/1288/1/012041